J|A|C|S
ARTICLES

Solvent Interactions and Conformational Choice in a Core *N*-Glycan Segment: Gas Phase Conformation of the Central, Branching Trimannose Unit and its Singly Hydrated Complex

E. Cristina Stanca-Kaposta,[†] David P. Gamblin,[‡] Emilio J. Cocinero,[†] Jann Frey,[†] Romano T. Kroemer,[#] Antony J. Fairbanks,[‡] Benjamin G. Davis,*[,‡] and John P. Simons*[,†]

Department of Chemistry, University of Oxford, Physical and Theoretical Chemistry Laboratory, South Parks Road, OX1 3QZ Oxford, United Kingdom, Sanofi-Aventis, CRVA, 13 quai Jules Guesde, BP14, 94403 Vitry-sur-Seine, France, and the Department of Chemistry, University of Oxford, Chemistry Research Laboratory, 12 Mansfield Road, OX1 3TA Oxford, United Kingdom

Received March 13, 2008; E-mail: john.simons@chem.ox.ac.uk; Ben.Davis@chem.ox.ac.uk

Abstract: The intrinsic conformational preferences and structures of the branched trimannoside, α-phenyl 3,6-di-*O*-(α-D-mannopyranosyl)-α-D-mannopyranoside (which contains the same carbohydrates found in a key subunit of the core pentasaccharide in *N*-glycans) and its singly hydrated complex, have been investigated in the gas phase isolated at low temperature in a molecular beam expansion. Conformational assignments of their infrared ion dip spectra, based on comparisons between experiment and ONIOM (B3LYP/6-31+G(d):HF/6-31G(d)) and single-point MP2 calculations have identified their preferred structures and relative energies. The unhydrated trimannoside populates a unique structure supported by two strong, central hydrogen bonds linking the central mannose unit (**CM**), and its two branches (**3M** and **6M**) closely together, through a cooperative hydrogen-bonding network: OH4(**CM**)→OH6(**3M**)→OH6(**6M**). A closely bound structure is also retained in the singly hydrated oligosaccharide, with the water molecule bridging across the **3M** and **6M** branches to provide additional bonding. This structure contrasts sharply with the more open, entropically favored trimannoside structure determined in aqueous solution at 298 K. In principle this structure can be accessed from the isolated trimannoside structure by a simple conformational change, a twist about the α(1,3) glycosidic linkage, increasing the dihedral angle ψ[C1(**3M**)−O3(**3M**)−C3(**CM**)−C2(**CM**)] from ∼74° to ∼146° to enable accommodation of a water molecule at the centrally bound site occupied by the hydroxymethyl group on the **3M** ring and mediation of the water-linked hydrogen-bonded network: OH4(**CM**) →OH_W→OH6(**6M**). The creation of a "water pocket" motif localized at the bisecting axis of the trimannoside is strikingly similar to the structure of more complex *N*-glycans in water, suggesting perhaps a general role for the "bisecting" OH4 group in the central (**CM**) mannose unit.

Introduction

Recent spectroscopic studies of carbohydrates in the absence of solvent have highlighted clearly delineated conformational landscapes which display well-defined minima,[1] but comparisons between the intrinsic, gas-phase structures of carbohydrates and their structures in aqueous solution have led to the conclusion that the inherent conformational preferences of oligosaccharides and consequently their secondary structures are modified by solvent interactions.[2,3] Molecular dynamics investigations of naturally occurring *N*-glycans in aqueous solution have identified enduring structural motifs supported by explicitly bound water molecules.[4] In such a scenario, questions arise as to the mechanism through which "bare" glycans acquire each solvent molecule. Is their acquisition specific and selective, and is there a midpoint of partial solvation that is a tipping point in the balance between inherent and solvated structural preferences? To what extent do the glycan structures that are selected by nature contain consistent pockets or "holes" for solvent?

Our earlier studies of hydration in small, unbranched glycans revealed a preference for water binding at weakly hydrogen-bonded OH sites which were "unpicked" by the solvent to create a stronger, cooperatively hydrogen-bonded network, often leading to conformational relaxation and a globally strengthened structure.[5,6] A key branched motif found in the core of most hydrated *N*-linked glycans could be strengthened by acceptance

[†] University of Oxford, Physical and Theoretical Chemistry Laboratory.
[#] Sanofi-Aventis, CRVA.
[‡] University of Oxford, Chemistry Research Laboratory.

(1) Simons, J. P.; Çarçabal, P.; Davis, B. G.; Gamblin, D. P.; Hünig, I.; Jockusch, R. A.; Kroemer, R. T.; Marzluff, E. M.; Snoek, L. C. *Int. Rev. Phys. Chem.* **2005**, *24*, 489–532.
(2) Kirschner, K. N.; Woods, R. J. *Proc. Natl. Acad. Sci. U.S.A.* **2001**, *98*, 10541–10545.
(3) Almond, A.; Sheehan, J. K. *Glycobiology* **2003**, *13*, 255–264.
(4) (a) Woods, R. J.; Pathiaseril, A.; Wormald, M. R.; Edge, C. J.; Dwek, R. A. *Eur. J. Biochem.* **1998**, *258*, 372–386. (b) Wormald, M. R.; Petrescu, A. J.; Pao, Y-L.; Glithero, A.; Elliott, T.; Dwek, R. A. *Chem. Rev.* **2002**, *102*, 371–386.
(5) Çarçabal, P.; Jockusch, R. A.; Hünig, I.; Snoek, L. C.; Kroemer, R. T.; Davis, B. G.; Gamblin, D. P.; Compagnon, I.; Oomens, J.; Simons, J. P. *J. Am. Chem. Soc.* **2005**, *127*, 11414–11425.

10.1021/ja801892h CCC: $40.75 © XXXX American Chemical Society
Published on Web 07/17/2008

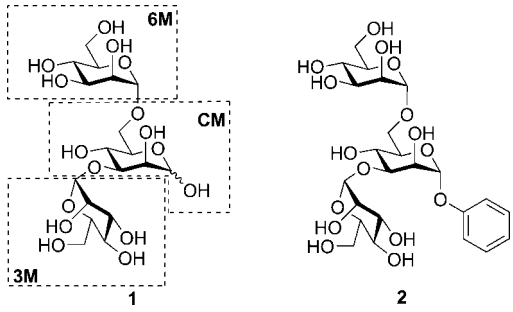

Figure 1. Branch point trisaccharide of structure **1** and its α-phenyl pyranoside derivative **2.** The labels **CM**, **3M**, and **6M** identify the different mannosyl residues as discussed in the text.

of a water molecule into its branch "fork". The recurrence of this site in many fully solvated glycan structures would suggest the existence of a "water pocket" in *N*-glycans that conserves a bisecting water molecule as a beneficial structural element, akin to the conserved water molecules found in lectin binding sites.[7]

In the past few years, it has become possible to determine experimentally the *intrinsic* conformational structures of carbohydrates isolated at low temperatures in the gas phase using a combination of vibrational spectroscopy, density functional theoretical (DFT), and *ab initio* calculation, and to identify the preferred structures and conformations of their hydrated complexes under the same conditions. These have revealed directly, their unperturbed conformational preferences and, perhaps more importantly, a role for water in modulating their structures, at least for the limited series of monosaccharides studied to date.[5,6] They have also revealed some correlation between the preferred water binding sites and those associated with protein−carbohydrate molecular recognition and led to a proposed set of "predictive rules" for both.[5]

The successful investigation of the intrinsic gas-phase conformations of two disaccharides, the α(1,3) and α(1,6) dimannosides[8] which correspond to the base sugars of the first two branches of the *N*-glycan, $Man_9(GlcNAc)_2$, has now led to the conformational analysis of the complete branch point in the representative trisaccharide, 3,6-di-*O*-(α-D-mannopyranosyl)-α-D-mannopyranose, **1** (which incorporates the α(1,3) and α(1,6) dimannoside units, see Figure 1), and also of its singly hydrated complex isolated at low temperatures in the gas phase. Valuably, its preferred conformation in aqueous solution at 298 K is already available through residual dipolar coupling NMR measurements by Prestegard and his co-workers[9] and Almond and Duus.[10] The conformational and structural assignments in the gas phase described here are based upon a combination of DFT, *ab initio*, and ONIOM[11] computation coupled with and also led by conformer-specific and mass-selective near-infrared (IR) vibrational spectroscopy, using the double resonance IR ion dip (IRID) detection strategy.

Methods

Vaporization. Transfer of the trimannoside into the gas phase followed essentially the same procedures described in an earlier investigation of its α(1,3) and α(1,6) dimannoside components.[8] Powdered samples were ground with graphite powder (graphite/trisaccharide mass ratio ≈ 1:10), deposited as a thin uniform surface layer on a graphite substrate, and placed in the vacuum chamber close to the exit of a pulsed, cylindrical nozzle expansion valve (0.8 mm diameter). Molecules were desorbed from the surface using the fundamental of a pulsed and focused Nd:YAG laser (2−4 mJ/pulse) and entrained and cooled in an expanding argon jet (∼4 bar backing pressure) before passing into the detection chamber through a 2 mm diameter skimmer. Hydrated complexes were formed by seeding the carrier gas with water vapor prior to the expansion (∼0.25% H_2O in Ar).

Spectroscopy. Conformer-specific IR spectra were recorded through a combination of mass-selected resonant two photon ionization (R2PI), double resonance IR−UV hole burning (HB) and IR ion dip (IRID) spectroscopy, following the procedures described earlier.[8] The individual IRID spectra provided the distinctive patterns of OH stretching modes through which the structural assignments could be made.

Computational Strategies. Conformational and structural assignments were performed through, and also led by comparisons between the experimental vibrational spectra and those determined through quantum chemical calculations on a wide range of conformers following procedures described earlier.[5,8] These were identified using a combination of force field conformational searches and quantum chemical calculations as implemented in the SYBYL (Tripos),[12] Macromodel,[13] and Gaussian 03[14] program packages, respectively.

Results, Discussion and Structural Assignments

The target phenyl mannoside **2**, designed as a representative minimal motif, contained two key features: the branch point of the *N*-glycan core and a "tag" chromophore needed for its detection and structural assignment via R2PI and IRID spectroscopy and provided by the phenyl group. The use of participating *O*-2 acetyl protection in the intermediate monomannosyl donor, **3** (Scheme 1), allowed excellently stereoselective (exclusively α) installation of the branch units **3M** and **6M**. Regioselective mannosylation of **7** at *O*-3 and *O*-6 was achieved through the use of regioselective pivaloylation at *O*-6 and *O*-3, protection of *O*-2 and *O*-4 as benzyl ethers, and subsequent removal of the pivaloyl esters. This protecting group controlled access to *O*-6 and *O*-3 proved to be a superior strategy to that based either on regioselective *O*-4 or *O*-2 protection via stannylene acetals or on direct regioselective *O*-3, *O*-6 bismannosylation methods.

Thus, the "branch point" trimannosyl unit, specifically phenyl 3,6-di-*O*-(α-D-mannopyranosyl)-α-D-mannopyranoside (**2**), was prepared by glycosylation of mannosyl diol acceptor **7** using two equivalents of mannosyl trichloroacetimidate donor **3** leading exclusively to the formation of *O*-6 and *O*-3 α-glycosyl linkages. The diol acceptor itself **7** was prepared by the reaction of benzyl mannoside **4** with two equivalents of pivaloyl chloride in pyridine at 0 °C which gave compound **6** in 56% yield

(6) Çarçabal, P.; Patsias, Th.; Hünig, I.; Liu, B.; Kaposta, E. C.; Snoek, L. C.; Gamblin, D. P.; Davis, B. G.; Simons, J. P. *Phys. Chem. Chem. Phys.* **2006**, *8*, 129–136.
(7) Toone, E. J. *Curr. Opin. Sruct. Biol.* **1994**, *4*, 719–728.
(8) Çarçabal, P.; Hünig., I.; Gamblin, D. P.; Liu, B.; Jockusch, R. A.; Kroemer, R. T.; Snoek, L. C.; Fairbanks, A. J.; Davis, B. G.; Simons, J. P. *J. Am. Chem. Soc.* **2006**, *128*, 1976–1981.
(9) (a) Sayers, E. W.; Prestegard, J. H. *Biophys. J.* **2000**, *79*, 3313–3329. (b) Tian, F.; Al-Hashimi, H. M.; Craighead, J. L.; Prestegard, J. H. *J. Am. Chem. Soc.* **2001**, *123*, 485–492.
(10) Almond, A.; Duus, J.Ø. *J. Biomol. NMR* **2001**, *20*, 351–363.
(11) (a) Maseras, F.; Morokuma, K. *J. Comput. Chem.* **1995**, *16*, 1170–1179. (b) Dappich, S.; Komaromi, I.; Byun, S.; Morokuma, K. J.; Frisch, M. J. *J. Mol. Struct.* **1999**, *451*, 1–21.
(12) *SYBYL 7.3*; Tripos International: St. Louis, Missouri.
(13) Mohamadi, F.; Richards, N. G. J.; Guida, W. C.; Liskamp, R.; Lipton, M.; Caufield, C.; Chang, G.; Hendrikson, T.; Still, W. C. *J. Comput. Chem.* **1990**, *11*, 440–467.
(14) Frisch, M. J.; et al. *Gaussian 03*, Revision B.03; Gaussian, Inc.: Pittsburgh, PA, 2003.

Scheme 1[a]

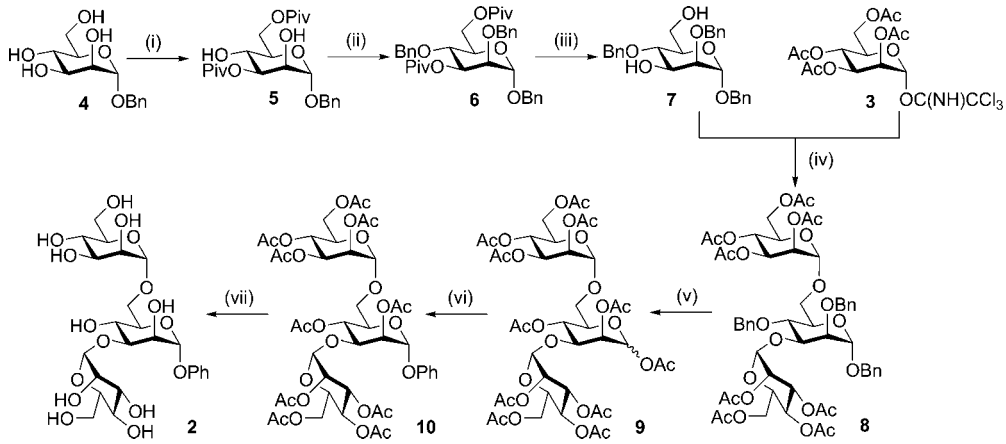

[a] (i) $(CH_3)_3CCOCl$, py, 0 °C, 56%; (ii) $BnOC(NH)CCl_3$, TMSOTf, DCM/cyclohexane, 70%; (iii) NaOMe, MeOH, reflux, 78%; (iv) $BF_3 \cdot OEt_2$, 4 Å MS, DCM, 75%; (v) H_2, $Pd(OH)_2$, EtOH then Ac_2O, py, 98% (2 steps); (vi) PhOH, $BF_3 \cdot OEt_2$, DCM, 74%; (vii) NaOMe, MeOH, 91%.

through regioselective esterification of *OH*-3 and *OH*-6 over *OH*-2 and *OH*-4. Subsequent benzylation on *OH*-2 and *OH*-4 could only be accomplished under mild Lewis acidic conditions with benzyl trichloroacetimidate to give **7** in 70% yield; base-assisted methods failed. Removal of pivaloyl protection using stoichiometric amounts of sodium methoxide in refluxing methanol gave diol acceptor **7**. The glycosylation reaction between the trichloracetimidate donor **3** and the diol acceptor **7** afforded the trisaccharide in 75% yield. Benzyl ether hydrogenolysis through treatment of **7** with Pearlman's catalyst ($Pd(OH)_2$) and hydrogen, followed by acetylation allowed protecting group exchange and gave peracetylated trimannoside **9**. The anomeric phenyl tag was introduced at this late stage on treatment of **9** with phenol and boron trifluoride diethyl etherate to furnish the phenyl α-mannoside **10**, in 74% yield. Global deacetylation gave the target tagged trisaccharide **2**.

Due to the large number of atoms in the phenyl trimannoside **2** and the high flexibility of the glycosidic linkages, the number of possible conformers is very high, and a full search of the conformational landscape would be correspondingly computationally expensive. A more efficient method allowed the *experiment* to guide the conformational search. Thus, several random conformational searches were carried out using different initial structures, and filtering of the relevant structures was performed based on the information obtained from the experimental infrared spectrum, which indicated the presence of cooperative hydrogen-bonded networks. The conformers resulting from the initial force field search were therefore scanned for such networks, including inter-ring hydrogen-bonding interactions, and the selected structures were then submitted for ONIOM calculations at the B3LYP/6-31+G(d):HF/6-31G(d) level (see Figure 2). Frequencies and relative energies for the most stable conformers were then calculated using the same ONIOM approach, but their relative zero-point corrected energies and free energies (at 298 K assuming harmonic frequencies) were evaluated through single-point calculations at the MP2/6-31+G(d) level. For comparison with the experiment, the O−H stretch frequencies were scaled by the factor 0.9734.

A similar procedure was applied to the water complex, where the experimental vibrational spectrum again guided the initial structures submitted for quantum chemical calculations. Several varieties of "prototype" structure were examined, incorporating a centrally sited water molecule, or a water molecule bound to OH groups located on the periphery or bridging across the

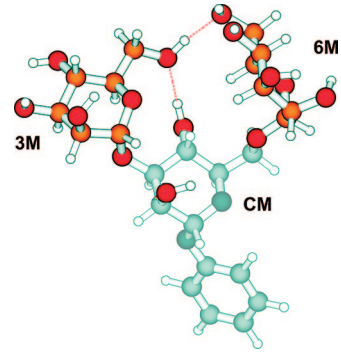

Figure 2. Description of the layers for the ONIOM (B3LYP/6-31+G(d):HF/6-31G(d)) calculations: the gray-colored atoms (phenyl tag and the central mannose (**CM**) sugar ring excluding the OH groups) were treated at the HF/6-31G(d) level, whereas the other atoms were treated at the B3LYP/6-31+G(d) level. The labeling identifies the mannose rings designated on the upper structure as **CM**, **3M**, and **6M** and discussed in the text.

mannose rings. The lowest-energy conformers obtained from the conformational search as well as representatives of the different prototype structures described above were submitted for higher level ONIOM (B3LYP/6-31+G(d):HF/6-31G(d)) geometry optimizations, frequency calculations, and MP2/6-31+G(d) single-point energy calculations, corrected for zero point and free energy, to identify their different IR signatures associated with alternative positions of the water molecule.

The experimental R2PI spectra of the phenyl trimannoside (**2**, TriMan) and its singly hydrated complex ($TriMan \cdot W_1$), both recorded in their mass selected parent ion channels, are shown in Figure 3. Apart from a small displacement, ~20 cm^{-1} to lower wavenumber in the hydrate they present very similar profiles, displaying a few sharp bands superimposed upon a broad underlying continuum and closely resembling the corresponding spectral profiles of the "phenyl tagged" α(1,3) and α(1,6) dimannosides.[8] Their associated vibrational (IRID) spectra, recorded in the O−H stretch region are shown in Figures 4 and 5. These both remained essentially the same when the UV probe was tuned across their R2PI spectra, indicating their predominant association in each case with a single structure only, and highlighting thereby a strong conformational preference in both the "bare" and the hydrated branching motifs. Furthermore, as for the dimannosides,[8] both the resolved features and the underlying continua in the two R2PI spectra must be

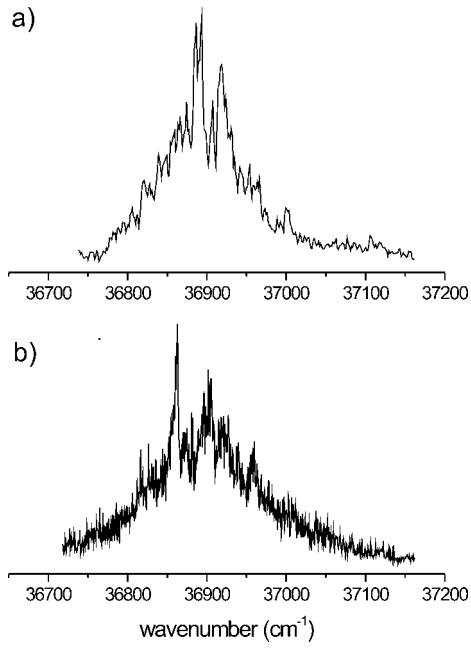

Figure 3. R2PI spectra of (a) TriMan **2** and (b) TriMan·W_1.

associated with the same carrier, which favors assignment of the unresolved background to the excitation of congested hot-band transitions.

The experimental IRID spectrum of TriMan is compared in Figure 4 with the ONIOM-computed vibrational spectra associated with several of its computed lowest energy and free energy conformational structures. Two of the computed spectra (parts d and e of Figure 4) are in remarkably good agreement with the experimental spectrum which presents two intense, strongly displaced and broadened bands at low wavenumbers, located at ~3400 cm^{-1} and ~3440 cm^{-1}, together with a cluster of bands lying at higher wavenumbers. Although their associated structures do not correspond to the lowest calculated energy, one of them lies close to the minimum free energy (calculated at 298 K). Given the flexibility of the trimannoside at the pre-expansion temperature and the theoretical approximations, the computed relative energies will be of less significance than the free energies,[15] and in any case the "true observable" is the vibrational spectrum.

The two conformers providing the best fit to experiment in TriMan present very similar structures and are held together by two central, co-operatively linked hydrogen bonds. They connect OH4 on the central mannosyl (**CM**) ring to the hydroxymethyl group on the α(1,3) mannosyl "wing", labeled **3M**, which is itself connected to the other hydroxymethyl group on the α(1,6) mannosyl "wing", labeled **6M**. Comparison between the experimental and computed spectra identifies the two strongly displaced bands as the symmetric (~3400 cm^{-1}) and antisymmetic (~3440 cm^{-1}) stretching vibrational modes associated with the central chain, OH4(**CM**)→OH6(**3M**)→OH6(**6M**). Thus, in the absence of water and at low temperature, the trisaccharide adopts a tightly bound "closed" conformation held together by strong intramolecular hydrogen bonds that link the component mannose units. The α(1,3) arm also preserves the conformational structure and bonding displayed in the α(1,3) dimannoside substructure **3M-CM** and in the corresponding conformer of the substructure **3M** monosaccharide, see Figure 6.[5,8]

Several alternative types of structural possibilities were envisaged for the singly hydrated trimannoside. The water molecule might bridge across the **3M** and **6M** branches (parts b and d of Figure 5) or across OH groups located on the periphery of the trisaccharide (Figure 5c), conserving the "closed" centrally hydrogen-bonded structure. Alternatively, the trimannoside framework might open up, for example by rotation of the **3M** wing about the α(1,3) glycosidic linkage (Figure 5e)

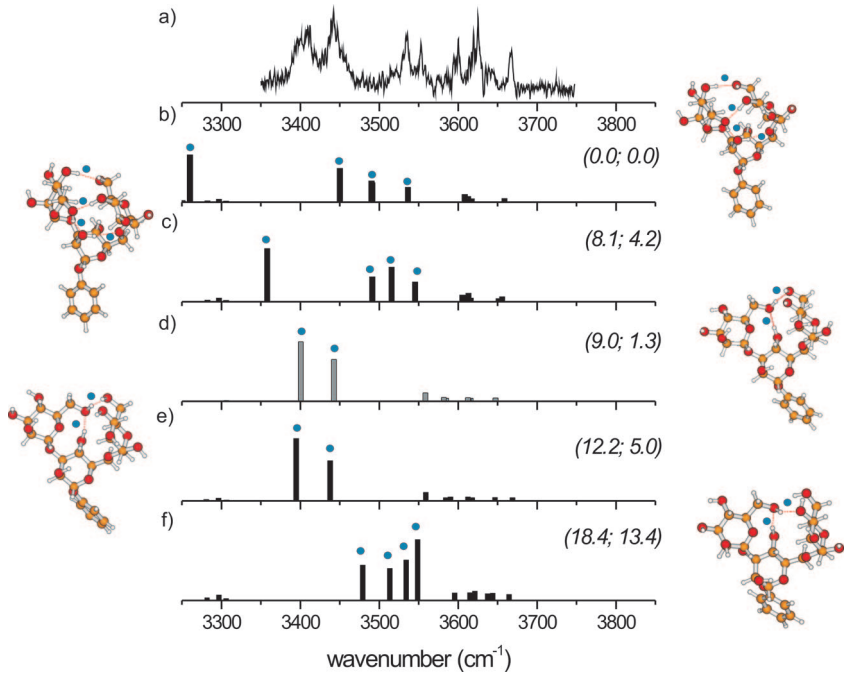

Figure 4. IRID spectrum of TriMan (a) and the predicted vibrational spectra (b, c, d, e, f) computed for its five lowest-energy conformers using the ONIOM (B3LYP/6-31+G(d):HF/6-31G(d)) approach; their structures are shown on both sides of the figure. The zero-point corrected relative energies and free energies at 298 K (in kJ mol^{-1}) calculated at the MP2/6-31+G(d) level are shown in brackets. The blue dots identify the strong hydrogen bonds in the structure and their corresponding features in the spectrum.

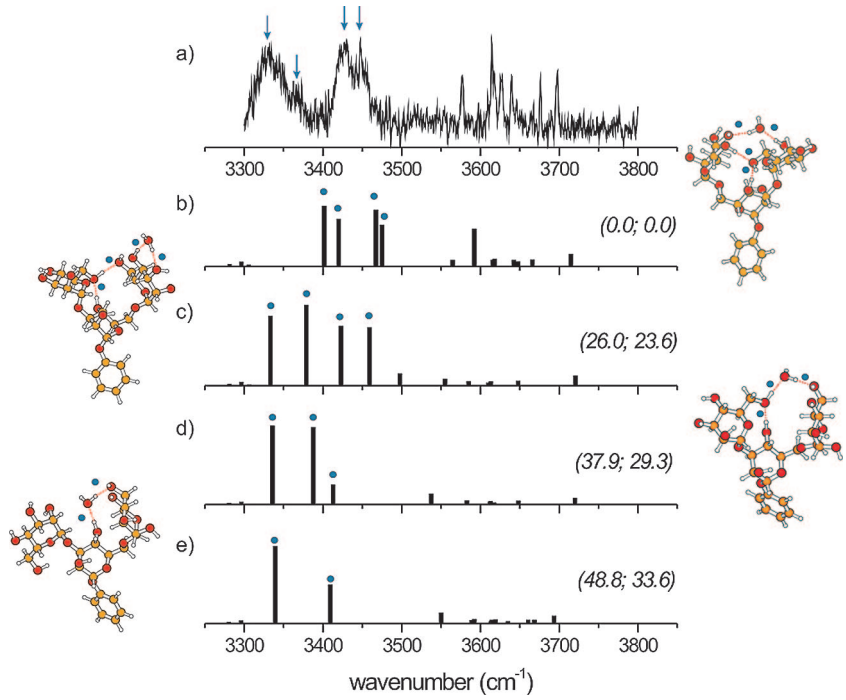

Figure 5. IRID spectrum of singly hydrated TriMan (a) and the vibrational spectra computed for alternative hydrated structures shown on both sides of the figure: (b) bridged I, (c) peripheral, (d) bridged II, and (e) central. Their zero-point corrected relative energies and free energies at 298 K (in kJ mol^{-1}) calculated at the MP2/6-31+G(d) level are shown in brackets. The blue dots and arrows indicate the two, three, or four strong hydrogen bonds in each class of singly hydrated TriMan structures and the corresponding features in the predicted and experimental spectra.

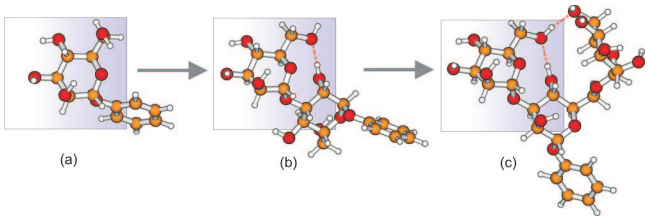

Figure 6. Schematic comparison between the determined conformational structures of (a) the α-mannoside monomer[5] **3M** (b) the dimannoside, Man α(1,3) Man **3M-CM**[8] and (c) the full trimannoside (**2**, TriMan) determined here. Despite variations in the contact partner, key features are maintained in the **3M** branch even as the complexity of the system increases.

allowing the water molecule into its interior to replace the central, hydrogen-bonded hydroxymethyl (**3M**) group and create the water-mediated chain, OH4(**CM**)→OH_W→OH6(**6M**). In two of these alternatives (parts b and c of Figures 5) the central intramolecular hydrogen bonds are complemented by two additional intermolecular H-bonds associated with insertion of the water molecule between two of the peripheral OH groups; this would lead to the appearance of four strongly displaced bands in the IR spectrum. The structure shown in Figure 5d would be signaled by the appearance of three strongly displaced bands, and in the centrally hydrated structure (Figure 5e) the two strong hydrogen bonds would be *replaced* by two new hydrogen bonds in which case the IR spectrum would continue to present two strongly displaced bands only.

The experimental IRID spectrum shown in Figure 5a actually presents two pairs of closely spaced, blended bands at low wavenumber, one presenting an asymmetric contour displaying a peak centered at ~3330 cm^{-1} and a subsidiary shoulder at ~3365 cm^{-1} and the other, two clearly defined peaks at ~3425 cm^{-1} and 3450 cm^{-1} in addition to the cluster at higher wavenumbers. Since the experimental IRID spectrum shown in Figure 5a displays four strongly displaced bands it must be associated either with a "peripheral" hydrate structure, for example insertion of the water molecule between OH4 and OH3 on the **6M** ring (Figure 5c), or with the structure shown in Figure 5b where the water molecule links the **3M** and **6M** rings. By good fortune, this structure (5b) also has the lowest calculated relative energy (at 0 K and free energy at 298 K, see Supporting Information for comparisons with other low-energy structures), and its computed IR spectrum is in good accord with that from experiment. It provides much the best agreement with the cluster of bands recorded at higher wavenumber, associated with the weakly H-bonded OH vibrational modes while the quartet at lower wavenumbers, associated with the more strongly H-bonded modes, presents a very similar pattern to the recorded spectrum. Indeed a slight increase in the "anharmonicity scaling" would bring the bands into very close accord, and it represents the most probable assignment.

Branched *N*-Linked Glycan Conformations in Aqueous Solution: Comparisons and Speculations. The "closed" conformational structures of the bare trimannoside and its singly hydrated complex displayed at low temperature in the gas phase contrast with the "open" structures determined in aqueous solution at 298 K, using NMR techniques coupled with MD calculations.[9,10] In the gas phase at low temperatures the preferred conformations of carbohydrates and their hydrated complexes are predominantly supported by cooperative intra- and intermolecular hydrogen bonding[4] as found for example in the present study: however, in aqueous solution at ambient temperatures in the absence of explicit solvation this may no longer be the case.[1,2] Nonetheless, it is notable that one of the set of computed singly hydrated structures, the centrally hydrated structure (Figure 5e) shown again in Figure 7a, adopts an (entropically favored) open conformation in remarkably close correspondence with that determined in aqueous solution. The

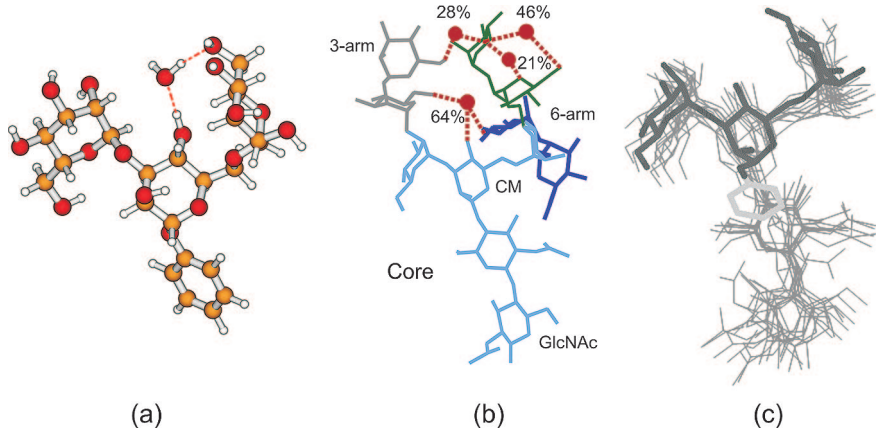

Figure 7. Comparison between (a) the computed open conformational structure of the monohydrate, TriMan·W1, (b) a snapshot of the $Man_9(GlcNAc)_2$ structure, including the preferred water binding sites together with their occupancy (in %) based on molecular dynamics calculations, and (c) the computed rmsd conformation of the core pentasaccharide segment, $Man_3(GlcNAc)_2$[16] based upon NMR measurements and MD simulations in aqueous solution at ~298 K[4] (black rods for the trisaccharide, light gray rods for the phenyl tag and gray thin wire frame) for the core pentasaccharide.

Table 1. Glycosidic Dihedral Angles of Phenyl Trimannoside in the Isolated and Singly Hydrated "Open" Form in the Gas Phase at Low Temperature and of Methyl Trimannoside in Aqueous Solution at ~298 K.

	ϕ, ψ (1,3)[a]	ϕ, ψ, ω (1,6)[b]
isolated	84, 74	71, 178, 60
"open" hydrate[e]	81, 146	69, 189, 60
aqueous[9]	60(80), −180(−100)	64, 180(60), 60(180)

	ϕ_H, ψ_H (1,3) [c]	ϕ_H, ψ_H, ω' (1,6)[d]
isolated	−34, −170	−46, 182, −64
"open" hydrate[e]	−35, −28	−47, 189, −64
aqueous[10]	−60, 0 ± 30	−60, 180, −60(60) ω'(−60):(60) = gg:gt ≈ 1

[a] ϕ[O5(i)−C1(i)−O3(i − 1)−C3(i − 1)]; ψ[C1(i)−O3(i)−C3(i − 1)−C2(i − 1)]. [b] ϕ[O5(i)−C1(i)−O6(i − 1)−C6(i − 1)]; ψ[C1(i)−O6(i)−C6(i − 1)−C5(i − 1)]; ω[O6(i)−C6(i)−C5(i)−C4(i)]. [c] ϕ_H[H1(i)−C1(i)−O1(i − 1)−C3(i − 1)]; ψ_H[C1(i)−O1(i)−C3(i − 1)−H3(i − 1)]. [d] ϕ_H[H1(i)−C1(i)−O1(i − 1)−C6(i − 1)]; ψ_H[C1(i)−O1(i)−C6(i − 1)−H6(i − 1)]; ω'[O6(i)−C6(i)−C5(i)−O5(i)]. [e] "Open" hydrated complex structure shown in Figure 7.

structure is generated by rotation of the **3M** wing in the bare molecule (shown in Figure 6c) about the dihedral angle ψ [C1(**3M**)−O3(**3M**)−C3(**CM**)−C2(**CM**)] associated with the α(1,3) glycosidic linkage, and insertion of the water molecule into its interior. The average dynamical values of the inter-ring glycosidic dihedral angles determined in aqueous solution at 298 K (unfortunately using different definitions for the dihedral angles ϕ, ψ (1,3) and ϕ, ψ, ω (1,6)) are listed in Table 1; they are remarkably close to the "frozen" dihedral angles in the open singly hydrated complex.

The angular orientation about the α(1,6) linkage, which retains a *gg* configuration in the gas phase both in the isolated trisaccharide and its generated hydrated complex, is also very similar to the corresponding average *gg* configuration in aqueous solution.

Even more striking comparisons can be made between the calculated structures of the open singly hydrated trimannoside unit (Figure 7a); the "water-bridged" structure of the high mannose *N*-glycan, $Man_9(GlcNAc)_2$ where the most persistent explicit hydration site incorporates a "keystone" water molecule H-bonded to OH4(**CM**) and two of the extended oligomannoside arms (Figure 7b);[4] and the average structure of its core pentasaccharide segment, $Man_3(GlcNAc)_2$. This is highlighted in Figure 7c which compares the "frozen" singly hydrated trimannoside structure (Figure 7a) with the computed rmsd structures of the core pentasaccharide unit stripped of its extended mannoside arms (based upon NMR measurements and MD simulations of the *N*-glycan in an aqueous environment at ~298 K).[4] The similarity between the open structure and the relative orientations of the **3M** and **6M** mannosyl "wings" in the trimannoside and in the corresponding unit in the core pentasaccharide is remarkable and provides some support for the conformation of the key branched (trimannoside) segment being driven by the creation of a water "pocket" in the branch "fork". Indeed in the absence of the extended mannoside arms—in the core pentasaccharide or the trimannoside—it would not be difficult for the central water molecule linked to OH4(**CM**) to slip into the water pocket. The repeated recurrence of this motif in many fully solvated glycan structures suggests a more general interplay between favored glycan structures and hydration, with water pockets that conserve bisecting water molecules acting as beneficial structural elements.

Acknowledgment. We thank Drs. Pierre Çarçabal, Bo Liu, Eoin Scanlan and Lavina Snoek for their contributions to the development and completion of this research. We are also grateful for the support provided by EPSRC, the Leverhulme Trust (Grant No. F/08788G), the Spanish Ministry of Education and Science (E.J.C.), the STFC Laser Loan Pool, the Oxford Supercomputing Centre and the Physical and Theoretical Chemistry Laboratory.

Supporting Information Available: Detailed description of the synthesis and characterization of **2**, **3**, **5**, **6**, **7**, **8** and **10**; Cartesian coordinates, total energies and larger-scale displays of the vibrational spectra and assignments of the conformations shown in Figures 4 and 5 and additional low-lying structures for the monohydrate; a table with all the structures for which the vibrational spectra are shown, displayed on a larger scale; and the complete ref 14. This material is available free of charge via the Internet at http://pubs.acs.org.

JA801892H

(15) Shubert, V. A.; Baquero, E. E.; Clarkson, J. R.; James, W. H., III; Turk, J. A.; Hare, A. A.; Worrel, K.; Lipton, M. A.; Schofield, D. P.; Jordan, K. D.; Zwier, T. S. *J. Chem. Phys.* **2007**, *127*, 234315.
(16) Kindly provided by M. R.Wormald.